Int. Agrophysics, 2004, 18, 217-223

INTERNATIONAL
Agrophysics
www.ipan.lublin.pl/int-agrophysics

Quantification of soil macroporosity with image analysis**

H. Czachor and J. Lipiec*

Institute of Agrophysics, Polish Academy of Sciences, Doświadczalna 4, P.O. Box 201, 20-290 Lublin 27, Poland

Received January 16, 2004; accepted February 18, 2004

A b s t r a c t. Identification and description of the size and shape characteristics of irregular and branched macropores helps the evaluation of the transmission functions of soil. Such macropores are usually formed by tillage operations. In this paper we present a methodological approach, based on the Aphelion image analysis package, to the identification of macropores and quantification of their size and shape characteristics such as surface area, perimeter, circularity, minimum bounding rectangle fill (MBR-Fill) and compactness of resin impregnated opaque sections. This approach includes division of branched macropores into smaller pores if the bottlenecks between them are narrow, assuming that they act independently. Two approaches were used to quantify pore radius from pore surface area (geometrical radius) and from the ratio of pore surface and perimeter (hydraulic radius). The first approach gave more reasonable results, because the hydraulic radius seems to be often poorly sensitive to the pore surface area. Moreover, the pore radius was calculated from the perimeter and it was considerably lower than that determined from the pore surface area. However, taking into account some pore shape characteristics improves the correlation between both radii. The presented approach may help in predicting transmission functions of soil.

K e y w o r d s: macropores, image analysis, pore splitting, pore radius

INTRODUCTION

Usually, macroporosity refers to pores bigger than 20-30 m that can be formed by soil tillage operations, soil fauna and roots of previous crops (Lipiec and Hatano, 2003). Their size can be up to some millimeters (Luxmoore, 1981; Ringrose-Voase, 1986).

Pore size distribution (PSD) of soil is often determined from the moisture retention curve (MRC) by means of Laplace relationship between the capillary pressure and equivalent pore radius (Walczak *et al*., 2002). It is necessary to emphasize four points of this classical approach:

1. MRC is an indirect method of PSD determination,
2. the term 'equivalent' introduces cylindrical shape of the capillaries,
3. when considering MRC we do not define the term 'a pore' *ie*, a single pore of the medium,
4. there is no possibility to quantify pores bigger than 100 micrometers by means of MRC.

The method of mercury intrusion porosimetry (MIP), frequently used to quantify pores less than 50 micrometers in size, possesses features similar to those of the MRC (Gliński *et al*., 1991; Pagliai *et al*., 2000; Sokołowska *et al*., 2001). The results of such measurements are used as input data in a physical model to predict the absolute movement of soil water. The agreement between models and observed behaviour has often been unsatisfactory due to inadequate pore data. In addition, both MRC and MIP are of limited applicability in respect to macropores which have a significant effect on the saturated water flow (preferential flow).

The image analysis approaches developed recently provide possibilities of deriving more accurate characteristics of soil macropore space. In this paper we propose a methodological approach for macropore identification and description, taking into account the size and shape parameters, using the Aphelion image analysis package.

MATERIALS AND METHOD

Soil sample preparation

Samples for analysis of soil pores were taken into metal containers (5 replicates) from the surface of soil in the horizontal plane 2-4 cm from the surface of cultivated Eutric Fluvisol with particles < 0.02 mm content at 48% w/w and

*Corresponding author's e-mail:hczachor@demeter.ipan.lublin.pl
**This work was partly supported by the State Committee for Scientific Research, Poland, Grant No. 3 P06R 001 23.

organic matter content of 2.3 % w/w (Puławy, Poland). After drying, the soil samples were saturated with a solution of Polimal 109 polyester resin. When hard, one surface of each block was polished with glass paper and powder to obtain opaque sections. A more detailed description of the procedure is in Słowińska and Domżał (1991).

The image acquisition was performed directly from the sections by means of a scanner with spatial resolution 0.195 mm. An example of a section is shown in Fig. 1. As the sizes of the sample were 7.8 x 8.3 cm, it is clear that some macropores (blacks) were bigger then 6-8 mm. Even a superficial look at the image shows a big diversity of sizes and shapes of the pores.

Image processing and analysis

A set of images, like that from Fig. 1, was processed by means of the Aphelion Image Analysis Package v.2.3. It allows for the processing, understanding and analysis to be performed independently from the source of image. The whole process is usually composed of several steps which utilize the following Aphelion groups of functions: Filtering, Edge detection, Segmentation, Mathematical morphology, Object processing. (Aphelion, 1997; Horgan, 1998; Czachor and Pawlak, 2001; Wojnar, 1999). The chosen operators with the appropriate parameters create a sequence called MACRO which allows the analysis of the investigated structure. Theoretically, each image requires an individual macro, but if a set of images concerns the same type of structure and the images have been acquired in the same conditions, one macro can be applied for all of them.

The macro developed for soil section analysis was composed of several operations. The input image from the scanner was composed of three-colour bands RGB: red (R), green (G), blue (B). It was split into 3 bands and the grey image with the best contrast was taken for further processing. The grey image of 256 hues was processed by applying the MaximumContrastThreshold operator to obtain a binary image (black-0, red-1), (Fig. 2). In the procedure, the operator picked a set of thresholds that gave maximum contrast and automatically selected thresholds that maximised the global average contrast of edges detected by the thresholds across the image (Aphelion, 1997).

Figure 2 shows the resulting image without pores smaller than 3.8 x 10^{-3}cm^2 which were eliminated for the reason of clearness of presentation. Application of such an image for the soil macropores description and for the prediction of permeability/water conductivity needs the answer to the question about the links between them. Intuitively, one would identify a pore as ‘a red island’ in Fig. 2. Even if the limits between the red clusters are frequently very narrow, their identification and visualisation can be done automatically by means of the Aphelion procedure called ClusterToLabels. It allows finding a set of pixels (cluster) which contact one another side-to-side (not corner-to-corner). Each cluster has its own colour as it can be seen in Fig. 3.

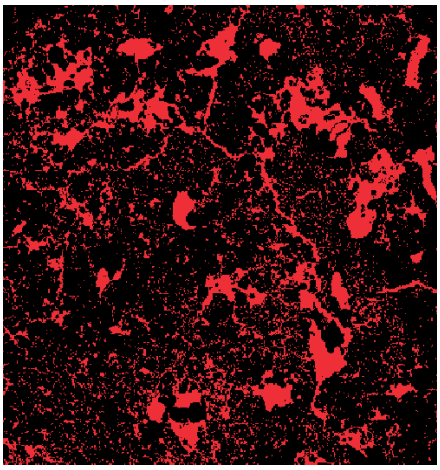

Fig. 2. Soil macropores found by means of the Maximum ContrastThreshold operator.

Fig. 1. Cross section of loess soil (A horizon, depth 10 cm) with macropores.

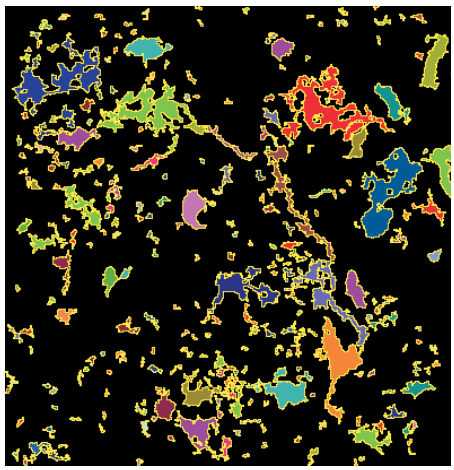

Fig. 2. Detection of soil macropores without splitting.

Determination of the macropore radius

The description of soil pores is often done via pore size distribution (PSD), where size is usually equal to the so called equivalent radius derived from MRC or MIP data. Neither of the methods is appropriate for macropores measurement.

The image analysis of soil sections is a useful method for quantitative description of the soil macropores. However, there is a fundamental difference between the MRC or MIP methods and the presented one. In this case, each macropore has to be first identified individually and then parameterised. Apparently, one can suppose the identity of the cluster from Fig. 3 and a single macropore. More careful section observation, however, suggests that such an approach seems to be unjustified. The pores in the image have a wide range of sizes and their shapes are far from circular. Two important features related to the considerable amount of clusters should be distinguished:

- some clusters have a solid inclusion (one or more) in one plane section,
- some bottlenecks linking a branch cluster are very narrow.

Both of them justify the division of such a cluster into two or more parts. Red colour in Fig. 4 shows an example of a pore from Fig. 3 which has both of the features mentioned. It is composed of several finger-like parts and some of them are practically separated from the others. Moreover, soil particles/aggregates can be found within the pore body. The approximation of such a shape by a circle of radius r calculated from surface area S is an approach that is frequently used:

$$r = \sqrt{S/\pi}, \tag{1}$$

but sometimes it can be too risky for the reasons mentioned above.

Fig. 4. An example of a big, branched cluster (red colour) from the upper right part of Fig. 3. The ellipse inscribed defines the Elongation parameter (Aphelion package) of the strongly concave cluster.

Hydraulic pore radius

Another possibility of parameterisation of pores with irregular shapes is provided by the method employing the hydraulic radius rH which is defined as the ratio of surface S and perimeter L (Singh and Mohanty, 2000):

$$rH = S/L. \tag{2}$$

However, the hydraulic radius rH of a figure composed of two or more parts connected by narrow bottlenecks is not sensitive in respect to the surface area, as can be seen from the calculations below. Let's imagine a pore composed of 2 adjacent circles of radii r_a and r_b. Firstly, one can assume it is one pore composed of two parts combined by a narrow neck. The cross-section area of such a pore is:

$$S = \pi\left(r_a^2 + r_b^2\right), \tag{3}$$

and its perimeter

$$L = 2\pi(r_a + r_b), \tag{4}$$

so, after substitution of 3 and 4 to 2, the hydraulic radius is:

$$rH = 0.5 r_a\,[1 + x - 2x/(1+x)], \tag{5}$$

where: $x = r_b / r_a$.

The relationship between the hydraulic radius of the composite pore rH and the radii ratio is shown in Fig. 5.

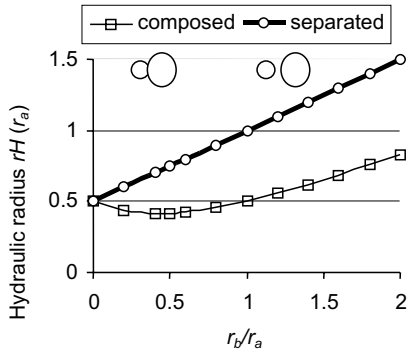

Fig. 5. Hydraulic radius of two clusters treated as one composite pore and two separated pores. Hydraulic radius for separated pores is the sum of the radii of both the pores.

On the other hand, the above mentioned two parts can be treated as two separate pores, and then:

$$s1 = \pi r_a^2, \tag{6}$$

$$s2 = \pi r_b^2, \tag{7}$$

and

$$L1 = 2\pi r_a, \tag{8}$$

$$L2 = 2\pi r_b, \tag{9}$$

where: $s1$, $s2$ – cross-section area of pores with radius r_a and r_b, respectively, and $L1$, $L2$ – perimeter of pores with r_a and r_b, respectively.

The hydraulic radius of the two pores rH_1 and rH_2 can be expressed as:

$$rH_1 = r_a/2, \tag{10}$$

and

$$rH_2 = r_b/2, \tag{11}$$

and their sum - rH_{1+2} – can be written as:

$$rH_{1+2} = r_a\,(1 + r_b/r_a)/2. \tag{12}$$

Equations (5) and (12) refer to the same objects: first treated as one pore, and then as two pores of the same total cross-section area.

It seems to be unexpected that function $rH = f(r_b/r_a)$ has a minimum. From the physical point of view, it signifies that the hydraulic radius of a composite pore can be smaller than the rH value related to its part. In particular, one can notice that two adjacent equal pores ($r_b/r_a = 1$) have the same rH value the as a single one ($r_b/r_a = 0$). Moreover, the hydraulic radius of a pore composed of several equal adjacent pores is the same as the value of a single one:

$$rH = n\,\pi\,r_a^2/(n\,2\,\pi\,r_a) = r_a/2. \tag{13}$$

Similar properties characterize a long pore – if its height is much smaller than width then its hydraulic radius is almost independent from the pore area.

Concavity and convexity of pores

Summarizing the above considerations, it is worth saying that both the methods presented can give the erroneous results of the equivalent radius of a concave pore - first one too big, the second – too small. One can predict that the division of a branched pore into smaller parts would increase the convexity of the resulting pores and give more reasonable permeability value of the soil. So the rising questions are:

- how to control the convexity-concavity of the pores and
- how to perform and control the splitting effect.

The Aphelion package offers a function called ImgConvexity which determines the value of convexity parameter equal to the number of the following configurations on a binary image (like Fig. 2):

0	0	0	0	0
0	1	1	1	0

where: 1 – pixels belonging to the object (pore), 0 – pixels outside of it. The above configuration detects convex objects when the convexity occurs at the top of them. This operation applied to the same image rotated by 90, 180, 270 degrees allows the total image convexity to be found, because it is equal to the number of entries in the objects, going from top to bottom. The concavity of an image is determined by means of the opposite configuration *ie* 0 replaced by 1 and 1 by 0.

Implementation and control of object splitting can be done be means of the morphological procedure called ClustersSplitConvex. A cluster is a set of connected pixels of the same value. If two parts of it contact via a bottleneck, then erosion can separate the cluster into two parts. If the size of the bottleneck is small with relation to the cluster parts being separated, than the effect of the separation is good. The power of separation can be tuned against the level above which a concavity creates a separation between two elements. The splitting effect of one pore for 3 levels of splitting power (100, 25, 24, respectively) is shown at Figs 4, 7, and 8. One (red) pore (Fig. 4) has been divided into 8 (Fig. 7) and 21 (Fig. 8) segments.

One can notice that solid intrusions in pores frequently promote splitting, and the newly created pore boundary lines go through them. This circumstance should be interpreted as a positive one, because the conductivity of such pores decreases dramatically in relation to 'empty' ones.

Figure 6 shows the convexity and concavity value of an image as a function of the splitting power of the Clusters SplitConvex procedure. Lower numbers correspond to higher levels of the splitting power. Both the concavity and convexity suddenly reverse their values for opposite when this parameter changes from 25 to 24.

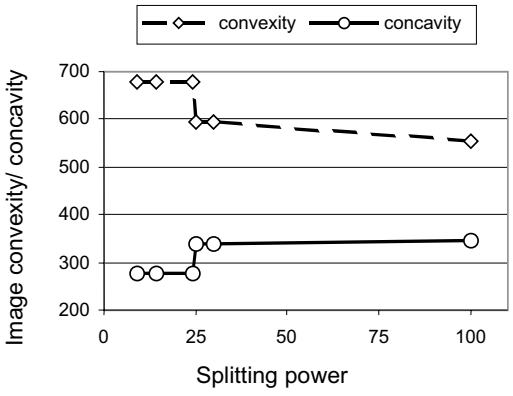

Fig. 6. Example of the convexity and concavity of an image vs. splitting power.

Pore size and shape parameters

The package used in this study calculates and saves a huge number of parameters of objects found. Some of them can be very useful for the description of soil pores. All of them can be divided into two groups:

- size parameters: Surface area, Crofton perimeter, MBR Height and Width, and others,

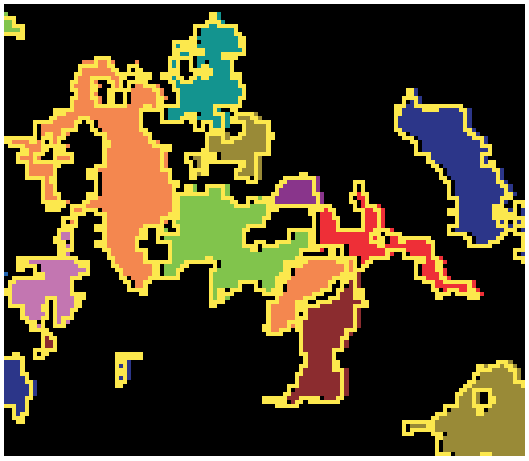

Fig. 7. Big pore from Figs 2 and 4 and the result of low power splitting procedure - 8 objects. The ellipse inscribed defines the Elongation parameter (Aphelion package) of the cluster.

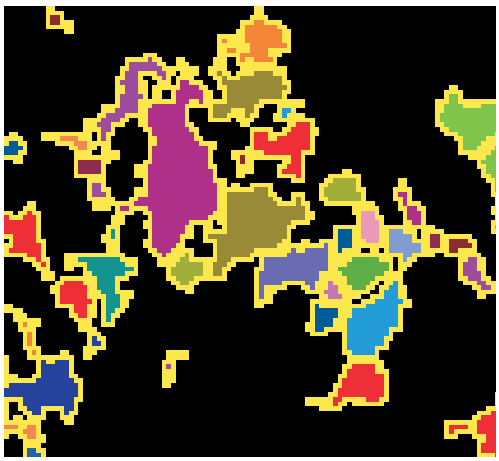

Fig. 8. Big pore from Fig. 2 divided into 21 objects as a result of high power splitting procedure.

- shape parameters: Elongation, Compactness, Circularity, MBR-Fill and many others.

The Crofton perimeter is a normalized count of the number of occurrences of 0, 45, 90, and 135 degree edges in the region. The 45 and 135 degree edges are normalized by √(2)/2).

The abbreviation MBR means Minimum Bounding Rectangle and refers to the rectangle of the smallest area containing the pore.

The above shape parameters are defined as follows:

- Compactness is 16 * Pixel-Count/(Perimeter^2).
- Elongation is the difference between the length of the major and minor axes of the best ellipse fit, divided by the sum of the lengths. This measure is zero for a circle and approaches one for an ellipse which is long and narrow.
- Circularity is (4 * Π * Area)/(Crofton-Perimeter^2).
- MBR-Fill is the ratio of pore and MBR area.

Some measurements on discrete (composed of pixels) space give results which are somewhat surprising. For example, the length of a staircase is always equal to the sum of the length and width of all the steps (irrespective of their size). An inclined line has such a character, and frequently its length is calculated according to the Crofton formula (Aphelion, 1997).

A majority of those parameters, especially shape one, work well with convex objects *ie* provide information about their geometry. In contrast, for example, Elongation related to the strongly concave pore from Fig. 4. (note the blue ellipse fitted in) does not characterise it at all. The same parameter determined for the pore in Fig. 7 reflects its shape more reasonably.

Summarising the above considerations concerning the splitting of concave pores, one can say that it provides a better characterisation of their geometry in relation to the soil properties.

The influence of splitting on pore frequency distributions can be estimated through the comparison of adequate relations. Figs 9-11 show the effect of splitting related to Crofton perimeter and MBR-Fill of the pores from Fig. 1.

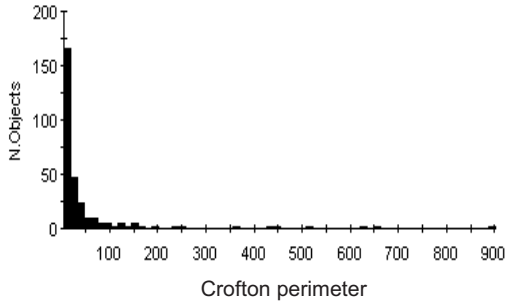

Fig. 9. Frequency distribution of the Crofton perimeter (see section Pore size and shape parameters) for non-split pores.

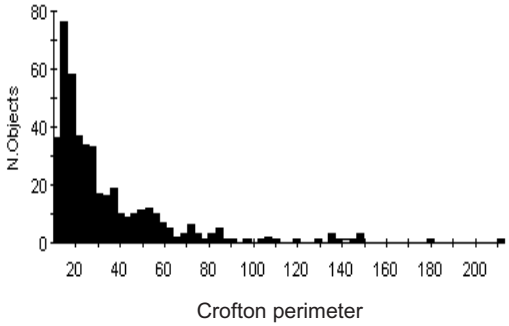

Fig. 10. Frequency distribution of the Crofton perimeter (see section Pore size and shape parameters) for split pores.

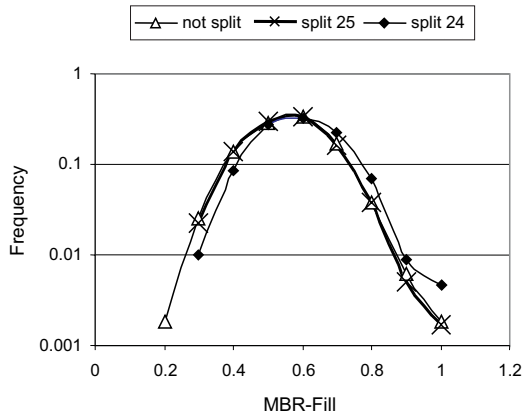

Fig. 11. Effect of pore splitting on the MBR-Fill (Minimum Bounding Rectangle Fill) frequency distribution.

T a b l e 1. MBR-Fill statistics for non-split and split pores

Pores	Minimum	Maximum	Mean	Stand. deviation
Not split pores	0.18	0.92	0.52	0.12
Split pores	0.27	1.00	0.56	0.11

One can notice that small pores dominate in the size distributions. However, the biggest pores occupy a relatively big part of the total porosity. Splitting caused a decrease in the variability range of both Area and the Crofton perimeter by a factor of 2 and 4, respectively. The influence of splitting on the MBR-Fill statistic for 350-400 pores is summarised in Table 1 and Fig. 11.

The mean value of MBR-Fill increased by 8%. The biggest change due to cluster splitting concerned the minimum value where the rectangle filling by a pore increased by 50% – from 0.18 to 0.27, as it can be seen in Fig. 11.

It was mentioned earlier that the correlation between r and rH is rather poor for concave pores. Pore radius r_1 can be calculated from the surface area (Eq. (1)) or from the pore perimeter value as:

$$r_2 = L/(2\pi). \tag{14}$$

T a b l e 2. Correlation between different pore radius estimators $r_1 = a\, r_2 + b$

r_1 ($S = \pi r_1^2$)	r_2 (L = $2\pi r_2$)	a	b	R^2
$\sqrt{(S/\pi)}$	S/L	0.21	0.31	0.79
$\sqrt{(S/\pi)}$	L/(2π)	2.19	-1.99	0.86
$\sqrt{(S/\pi)}$ (MBR-Fill)^2	S/L	1.08	-0.22	0.85
$\sqrt{(S/\pi)}$	2 S/(L $\sqrt{}$(CIRC))	1.00	0	1.00
$\sqrt{(S/\pi)}$	L/(2π) MBR-Fill	1.05	-0.65	0.95

For circular pores both r_1 and r_2 values should be equal. Table 2 shows some relationships between pore radii (r_1 and r_2) calculated from the pore surface (S) and the pore perimeter (L), and selected shape parameters (MBR-Fill and Circularity). One can notice that the pore radius deter- mined from the surface area (S) is more than twice as big as that calculated from the Crofton perimeter (L) (second line in Table 2). Perfect agreement $R^2 = 1$ between the geometrical radius and 2 S/(L $\sqrt{}$(Circularity)) is quite natural (see Circularity definition). Moreover, the MBR_Fill parameter seems to be very useful for the description of actual irregular pores.

The above data indicate the possibility of different approaches to pore characterisation when looking for the relationship between pore distribution and the physical properties of soil. The results concerning the geometrical r and hydraulic rH radii are shown in Figs 12 and 13, where the cumulative pore surface area distribution (CPAD) is defined as:

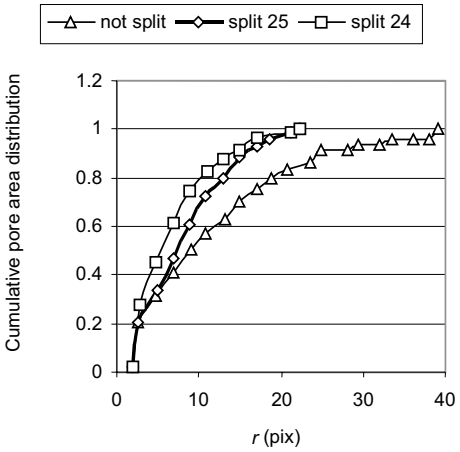

Fig. 12. Cumulative pore surface area distribution vs. geometrical radius r for 3 levels of pore splitting.

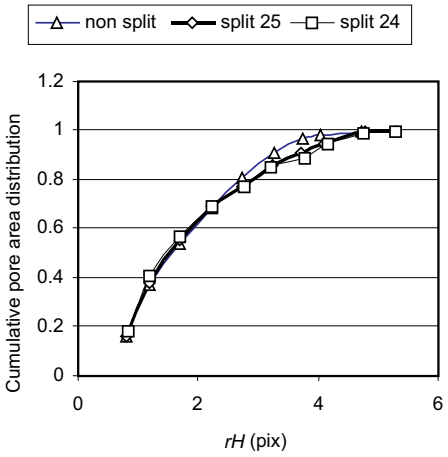

Fig. 13. Cumulative pore surface area distribution vs. hydraulic radius rH for 3 levels of pore splitting.

$$CPAD = \pi \sum_{i=1}^{n} p_i r_i^2 / S, \quad (15)$$

where: p_i – percent contribution of pores of radius r_i, S – total surface area of all pores.

Some features of the characteristics presented look surprising: for example, the range of hydraulic radius values of split pores is greater than for non-split ones. Generally, the differences between the cases investigated are much smaller in relation to the geometrical radius *r*, which can be explained as the consequence of the hydraulic radius features that have been described earlier.

The above results concern the set composed of 1600-2100 pores which have been found in 5 images of loess alluvial soil (A horizon, depth 10 cm). Pores with a surface area smaller then 10 pixels (3.8×10^{-3} cm^2) were not analysed because their shapes were not precisely determined (scanner spatial resolution equals 0.0195 cm). The width of the smallest pore is 500-600 m.

MRC provides information on pores of equivalent diameter of up to about 100 m. The method presented herein can be considered as complementary to MRC because it allows the analysis and quantification of pores of much larger diameter.

CONCLUSIONS

1. Detected sets of connected pixels (clusters) cannot be identified as single pores when their shape is concave or solid intrusions can be found inside.

2. It was proposed to split such big concave clusters into sets of more or less convex single pores by means of the Aphelion ClusterSplitConvex procedure.

3. Quantification of the pore radius based on the pore surface area (geometrical radius *r*) compared to its calculation from the ratio of the surface area and the perimeter (hydraulic radius *rH*) gives more reasonable results. This is due to the hydraulic radius showing a relatively weak correlation to the pore surface area.

4. Pore radius can be calculated from its perimeter as well as if some shape parameters (MBR-Fill or Circularity) are taken into account.

REFERENCES

Aphelion Image and Understanding Software, version 2.3i, ADCIS and AAI Inc., **1997**.

Czachor H., Konstankiewicz K., Pawlak K., and Wojnar L., 2000. Application of image analysis for quantification of potato tuber tissue. 6th Int. Conf. Stereology and Image Analysis in Material Science, STERMAT 2000, Kraków, 301-306.

Gliński J., Konstankiewicz K., Moreno F., and Stawiński J., 1991. Macroscopic and porosimetric analysis of soil under different tillage methods and compaction. Polish J. Soil Sci., 34(2), 211-221.

Horgan G.W., 1998. Mathematical morphology for analysing soil structure from images. Eur. J. Soil. Sci., 49, 161-173.

Lipiec J. and Hatano R., 2003. Quantification of compaction effects on soil physical properties and crop growth. Geoderma, 116, 107-136.

Luxmoore R.J., 1981. Macro- meso- and microporosity of soil. Soil Sci. Soc. Amer. J., 45, 671-672.

Pagliai M., Pellegrini S., Vignozzi N., Rousseva S., and Grasselli O., 2000. The quantification of the effect of subsoil compaction on soil porosity and related physical properties under conventional to reduced management practices. In: Subsoil Compaction - Distribution Processes and Consequences. (Eds Horn R., van den Akker J.J.H., Arvidsson J.). Catena, 32, 305-313.

Ringrose-Voase A.J., 1996. Measurement of soil macropore geometry by image analysis of section through impregnated soil. Plant and Soil, 183, 27-47.

Singh M. and Mohanty K.K., 2000. Permeability of spatially correlated porous media. Chem. Eng. Sci., 55, 5393-5403.

Słowińska-Jurkiewicz A. and Domżał H., 1991. The structure of the cultivated horizon of soil compacted by the wheels of agricultural tractors. Soil Till. Res., 19, 215-226.

Sokołowska Z., Hajnos M., Hoffmann C., Renger M., and Sokołowski S., 2001. Comparison of fractal dimensions of soils estimated from adsorption isotherms, mercury intrusion and particle size distribution. J. Plant Nutr. Soil Sci., 164, 591-599.

Walczak R., Witkowska-Walczak B., and Sławiński C., 2002. Comparison of correlation models for the estimation of the retention characteristics of soil. Int. Agrophysics, 16, 79-82.

Wojnar L., 1999. Image Analysis, Application in Materials Engineering. CRC Press LLC, Boca Raton, USA.